Available online at www.sciencedirect.com

Organic Electronics 4 (2003) 131–141

Organic Electronics

www.elsevier.com/locate/orgel

The influence of a PEDOT:PSS layer on the efficiency of a polymer light-emitting diode

A. van Dijken, A. Perro, E.A. Meulenkamp, K. Brunner *

Philips Research Laboratories Eindhoven, Prof. Holstlaan 4, 5656 AA Eindhoven, The Netherlands

Abstract

The mutual influence of the constituent layers in a polymer light-emitting diode on the photoluminescence quantum efficiency of the light-emitting polymer is investigated. It is shown that a specific chemical interaction can occur between poly-(3,4-ethylenedioxythiophene):poly-(styrenesulphonic acid) (PEDOT:PSS) and poly-(*p*-phenylenevinylene) (PPV). It is further shown that PEDOT:PSS has a considerable effect on molecular dopants dispersed in the polymeric host. In the case of PPV the interaction with PEDOT:PSS results in the creation of defect states in an interface region between the PEDOT:PSS layer and the PPV layer. The presence of these defect states results in a considerable quenching of the PPV photoluminescence. For devices based on PPV, already at voltages below the built-in voltage the PEDOT:PSS-induced defect states can be filled with charge carriers, a process that can be monitored with field-dependent photoluminescence measurements and with electrical impedance measurements. Filling of defect states with charge carriers constitutes a dynamic photoluminescence quenching mechanism, that is present in addition to the previously mentioned static quenching mechanism due to the presence of defect states. As a result, the photoluminescence intensity of PPV in a working device under operating conditions can be quenched by at least 20% with respect to the intensity at zero applied volt. To indicate that these effects involve a specific interaction between PEDOT:PSS and PPV, it is shown that the effects are absent in devices based on poly-(2,7-spirofluorene) (PSF) instead of PPV, and that the effects are independent of the type of cathode material. Defect states in PPV can be created through an electrophilic addition reaction involving the PPV vinylene bond and protons from PEDOT:PSS.

1. Introduction

The light-emitting layer in a polymer light-emitting diode (pLED) is the centerpiece of the device. Several functions such as charge injection, charge transport, and exciton formation are combined in this single layer. The characteristics of the light-emitting polymer (LEP) broadly define the limits to the internal quantum efficiency, the emission color, and put constraints on the choice of electrodes. Obviously, interactions of the LEP with other layers in the device can play an important role. Chemical reactions and exciton quenching by the electrodes, for example, depend on the choice of materials adjacent to the LEP. Thus, the LEP as it is present in a pLED under operating conditions truly determines device properties such as efficiency and lifetime.

State-of-the-art pLEDs contain a layer of a conducting polymer between the anode and the LEP which acts as a hole injection layer. This

---

* Corresponding author.

E-mail address: klemens.brunner@philips.com (K. Brunner).

1566-1199/$ - see front matter © 2003 Elsevier B.V. All rights reserved.
doi:10.1016/j.orgel.2003.08.007

conducting polymer is usually poly-(3,4-ethylenedioxythiophene):poly-(styrenesulphonic acid) (PEDOT:PSS). In this paper, the influence of PEDOT:PSS on the photoluminescence (PL) efficiency of the LEP is studied. Steady-state PL measurements are used to determine the relative quantum efficiency of LEP layers which have or have not been in contact with PEDOT:PSS. To study the effect of PEDOT:PSS on the efficiency of a pLED under electrical operation, field-dependent PL measurements are performed on working devices with and without a PEDOT:PSS layer. Finally, in order to gain more insight into the nature of the interaction between PEDOT:PSS and LEP, electrical impedance measurements are performed.

In the newest generation of pLEDs the light-emitting layer can be a mixture or co-polymer of a host polymer and guest molecules [1–5] (which we will continue to denote by LEP for the sake of clarity). Such a material system enables a particularly appealing solution to fabrication of full-color graphic displays with pLED technology because the color can be adapted through energy transfer or charge transfer from the host polymer to emissive guest molecules, without major changes in the material synthesis and processing. Thus, the interaction of PEDOT:PSS with a blue-emitting poly-(2,7-spirofluorene) (PSF) host is studied and compared to that of the archetypal electroluminescent polymer, poly-(*p*-phenylenevinylene) (PPV).

Recently, research on new materials for organic electroluminescent displays has started to look at the use of phosphorescent emitters, which give an increase in the efficiency through harvesting of the triplet states [6–8]. This research has stimulated the development of electroluminescent heavy metal complexes [9,10]. The electrical and photophysical properties of molecular dopants can be very sensitive to their environment [11]. This is especially true for the heavy metal complexes. Therefore, possible interaction of PEDOT:PSS with an iridium-based dye, a typical representative of this class of molecules, has been investigated.

The results underline the importance of determining the photophysical and electrical properties of the LEP in actual working devices as there can be a marked difference in e.g. PL quantum efficiency for layers deposited on glass, in a device at open-circuit voltage, and at operating voltage. We also give an example of changes during constant current driving of a pLED that are due to the presence of a PEDOT:PSS layer.

2. Experiment

Polymer light-emitting diodes were fabricated under clean room conditions using pre-cleaned indium–tin oxide (ITO) coated glass substrates. The ITO was treated in a UV/O_3 photoreactor and remaining dust particles were blown away with ionized nitrogen. In some experiments a hydrogen plasma treatment (1 min 340 W; 0.28 mbar H_2 pressure) followed the UV/O_3 cleaning step. Polymer solutions were filtered through a 5 μm filter and spin-coated using a BLE Delta 20 BM.

Two types of devices were fabricated: (a) single-layer devices, and (b) double-layer devices. Single-layer devices consist of only a LEP layer (80 nm unless mentioned otherwise) sandwiched between two electrodes. In double-layer devices a layer of PEDOT:PSS, 1:6 dispersion in water, electronic grade AI4083, HC Starck [12,13]) is used (200 nm unless mentioned otherwise). PEDOT:PSS layers were annealed at 180 °C for 2 min. LEPs based on PPV (Covion Organic Semiconductors GmbH [14,15], see Fig. 1) and poly-(2,7-spirofluorene) (PSF, Covion Organic Semiconductors GmbH [16], see Fig. 1) were used. Metal cathodes were applied by vacuum evaporation through a mask and consisted of either Au or Ba/Al (5 nm Ba capped with 100 nm Al). The work function of Au is high (5.3 eV [17]) and as a result no electrons can be injected into the LEP at the applied voltages used in the experiments described in this paper. Thus, with a Au cathode, a unipolar device is obtained in which the current is being carried by holes only. A bipolar device is obtained with Ba/Al as cathode material as the work function of Ba is such (2.7 eV [17]) that electrons can be easily injected into the LEP. The devices were fabricated in a nitrogen atmosphere inside a glove box ($[O_2]$, $[H_2O]<1$ ppm). Before the devices leave the glove box, they are encapsulated with a metal lid to

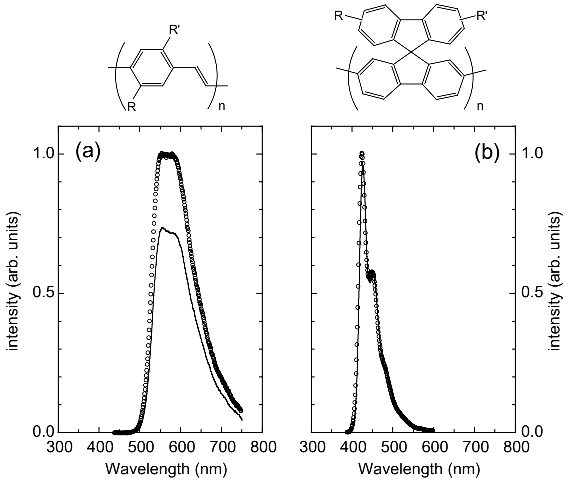

Fig. 1. Normalized PL spectra of 100 nm layers of (a) PPV and (b) PSF on glass. The open circles represent the spectra as obtained on layers from H_2O-treated polymers. The solid lines represent the spectra as obtained on layers from PEDOT:PSS-treated polymers. The PPV and PSF luminescence was excited at 410 and 380 nm, respectively.

prevent oxygen and water from degrading the device performance. A getter is also included in the encapsulated devices.

Layer thicknesses were determined using a Dektak^3 ST surface profile measuring system. Steady-state PL spectra were measured in ambient atmosphere using a Perkin–Elmer LS 50B spectrometer. The emission spectra were corrected for the spectral response of the emission monochromator and the photomultiplier tube. PL spectra of single LEP layers were measured on plain glass substrates. PL spectra of LEP solutions were measured using 1 mm quartz cuvettes. The spin-coated samples were prepared under nitrogen atmosphere inside a glove box. By measuring the samples immediately after transfer from the glove box and by keeping the measurement time short, care was taken that the measurements did not suffer from oxidative degradation of the polymer [18]. The samples were always photo-excited at the LEP side. Field-dependent PL intensity was monitored at the peak emission wavelength using 350 nm excitation. The emission and excitation spectra were independent of bias in the voltage range of interest here. PL was separated from EL under forward bias by flash excitation and time-gated emission integration.

Electrical impedance measurements were performed using a Schlumberger SI 1260 impedance/gain-phase analyzer. The impedance is measured by applying a sinusoidally varying voltage modulation (rms amplitude 30 mV), superimposed on a constant dc voltage. The frequency of the voltage modulation and the value of the dc voltage were varied from 10 to 10^6 Hz and from -2 to 5 V, respectively. Fits of the impedance data to equivalent circuits were performed using the software program ZView (version 2.4a, Scribner Associates, Inc.).

3. Results

3.1. Photoluminescence

3.1.1. Pristine polymers

The PL intensity of LEP layers spin-coated directly on plain glass substrates (single-layer samples) was compared to that of the same LEP layers spin-coated on a PEDOT:PSS layer on glass (double-layer samples). Both the PEDOT:PSS layer and the LEP layer had a thickness of 100 nm. PPV and PSF photoluminescence spectra from several samples were averaged and integrated. The absorbance of the sample and the shape of the PL spectrum were not influenced significantly by the PEDOT:PSS layer. Hence, the measured PL intensity was, to a good approximation, proportional to PL efficiency. It was found that the PL efficiency of a double-layer PPV sample with PEDOT:PSS is reduced by about 40% as compared to a single-layer PPV sample without PEDOT:PSS. The PL efficiency of PSF was not influenced by the presence of a PEDOT:PSS layer (data not shown here).

In this first series of experiments, the absolute change in the PL efficiency due to the presence of a PEDOT:PSS layer remains somewhat uncertain because of possible changes in in-coupling and out-coupling of excitation and emission light, respectively. Although this complication would hardly affect the noted marked difference between PSF and PPV, a second series of experiments was performed, which rules out optical effects as the origin of the PL quenching of PPV, leaving chemical interactions as the only possible mechanism.

Solutions of LEPs in toluene (mass-to-volume fractions of 0.45% and 0.75% for PPV and PSF, respectively) were mixed with an aqueous solution of PEDOT:PSS and vigorously stirred for 1 h. After phase separation of the toluene/water emulsion, part of the organic phase (containing only LEP and no PEDOT:PSS) was used for a PL measurement and part was used to spin-coat a layer (of thickness 100 nm) on plain glass. In this way, a single-layer sample of a PEDOT:PSS-treated LEP was obtained. For reference samples the same procedure was followed except that the aqueous PEDOT:PSS solution was replaced by purified water (single-layer sample of a H_2O-treated LEP).

Fig. 1 contains the PL spectra of the single-layer samples (all having the same layer thickness, viz. 100 nm). A similar trend as mentioned above for the single-and double-layer samples is observed: no difference in PL intensity between PEDOT:PSS-treated PSF and H_2O-treated PSF, while the PL intensity of PEDOT:PSS-treated PPV was reduced by about 30% as compared to H_2O-treated PPV.

3.1.2. Molecularly doped polymers

In a previous publication it was established that the electro- and photoluminescence of certain electron donor-bridge-acceptor systems used as emitter in a poly-(*N*-vinylcarbazole) (PVK) matrix, was completely quenched in the presence of PEDOT:PSS [11]. Only when the thickness of the LEP layer was increased to 140 nm, could part of the luminescence of the molecular dopant dispersed in the LEP layer be retained. A similar result was obtained when PSF was used instead of PVK [19].

In this paper, the investigation of the influence of PEDOT:PSS on molecular dopants is extended to a class of highly efficient triplet emitters introduced by Baldo et al. [7]. The orange-red light-emitting iridium(III) bis(2-phenylquinolyl-N, $C^{2\prime}$) acetylacetonate ($Ir(pq)_2(acac)$) [9,10] was dispersed in PSF (mass fraction of 5%) and double-layer devices consisting of a PEDOT:PSS layer and a molecularly doped PSF layer were constructed. The devices showed emission from $Ir(pq)_2(acac)$ only, at efficiencies typical for this particular triplet emitter. Standard device lifetime measurements were conducted at an initial luminance of 200 cd/m^2. The measured lifetime (defined as the time at which the luminance has decreased to half of its initial value under constant current driving) was considerably shorter for $Ir(pq)_2(acac)$ than for a typical orange-red singlet emitter. After lifetime, the emission of $Ir(pq)_2(acac)$ is quenched by almost 80% and no PSF emission is recovered (see Fig. 2). Additionally, a new emission band has appeared at about 480 nm. The same emission band is also observed when an organic solution of

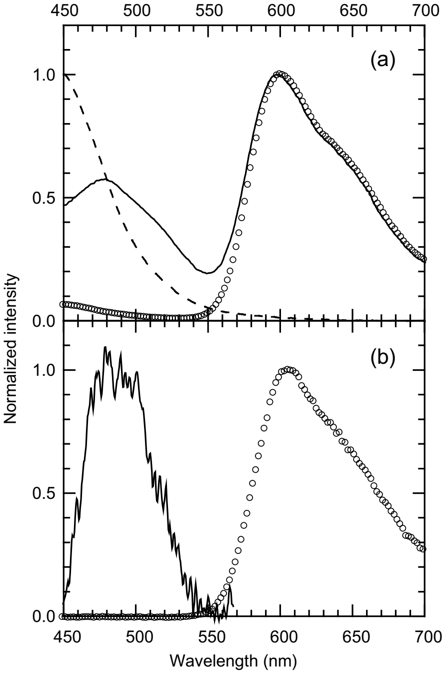

Fig. 2. (a) PL of a double-layer pLED containing a PEDOT:PSS layer and a layer of PSF in which $Ir(pq)_2(acac)$ is dispersed at a mass fraction of 5%, before (open circles) and after (solid line) device lifetime. As a reference, the PL spectrum of a device with undoped PSF after lifetime is also shown (dashed line). The spectra are normalized at the maximum of the $Ir(pq)_2(acac)$ emission band. (b) PL of an organic solution of $Ir(pq)_2(acac)$ before (open circles) and after (solid line) interaction with PEDOT:PSS. The spectra are normalized at the maximum emission intensity.

$Ir(pq)_2(acac)$ is treated with an aqueous solution of PEDOT:PSS, analogous to the procedure described above.

Fig. 2 provides further evidence that PEDOT:PSS can have a considerable influence on the performance of the LEP. In a way, molecular dopants such as the electron donor-bridge-acceptor system and the triplet emitter, can be seen as a sensitive probe for the interaction of PEDOT:PSS with the LEP. In a double-layer device, an interface region exists where PEDOT:PSS is in contact with the LEP. As the emission of $Ir(pq)_2(acac)$, when dispersed in a LEP layer, quenches during operation of the device and an additional emission band appears, either the $Ir(pq)_2(acac)$ migrates into the interface region or the boundary of the interface region progresses into the LEP layer. From the thickness dependence of the emission efficiency of the donor-bridge-acceptor system it can be concluded that the influence of the PEDOT:PSS layer gradually decreases when the LEP layer thickness increases.

3.1.3. Field-dependent photoluminescence

The field-dependence of the photoluminescence of bipolar PPV devices with and without a PEDOT:PSS layer is compared in Fig. 3. Open squares refer to H-plasma-treated ITO. This has a work function which is about 0.5 eV lower than that of UV/O_3-treated ITO and PEDOT:PSS (the work function is approximately 5.0 eV for the latter according to contact potential difference measurements). H-plasma treated ITO acts as a poor hole injector, leading to a lower current and a considerably lower EL efficiency. The built-in voltage (V_{BI}) is about the same for all three samples.

At negative applied voltage, the field-dependence of the PL intensity is identical for all types of devices. The decay in PL efficiency is due to electric field-induced exciton dissociation [20–22] and is not influenced by the choice of anode or ITO pretreatment. Indeed, it was found that quenching at large reverse voltage occurs at the same internal field for a LEP thickness range from 34 to 110 nm (see Fig. 4).

The situation is entirely different at small negative voltage and around V_{BI}, where noticeable differences in PL field-dependence are clearly visible. The single-layer PPV device with a

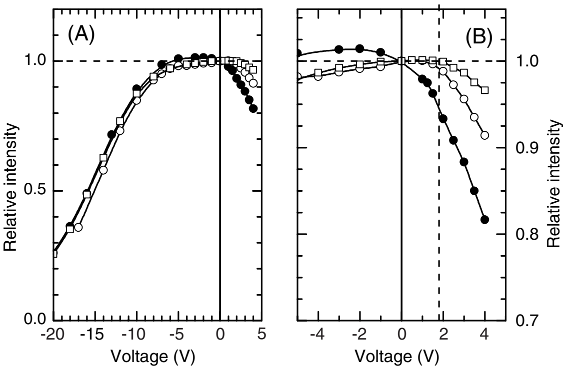

Fig. 3. PL intensity (normalized to the intensity at 0 V) as a function of applied voltage for bipolar PPV devices. Three different devices are shown: a single-layer device with H-plasma-treated ITO (open squares), a single-layer device with UV/O_3-treated ITO (open circles), and a double-layer device with UV/O_3-treated ITO and a PEDOT:PSS layer (solid circles). The PL intensity over the entire voltage range is shown in (A) while (B) contains only the data obtained between −5 and +5 V. The solid lines are guides to the eye. The vertical dashed line in (B) indicates the built-in voltage (V_{BI}) of the devices.

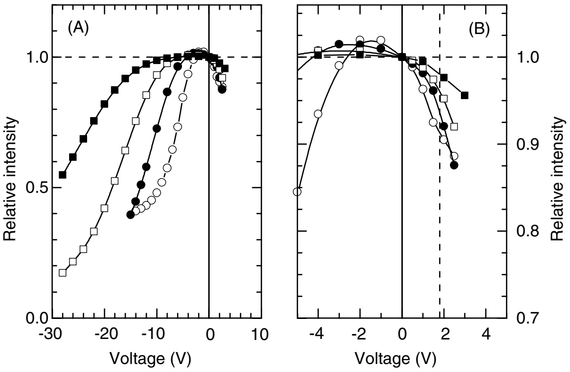

Fig. 4. PL intensity (normalized to the value at 0 V) as a function of applied voltage for bipolar double-layer PPV devices having different PPV layer thickness: 34 nm (open circles), 56 nm (solid circles), 78 nm (open squares) and 110 nm (solid squares). The PL intensity over the entire voltage range is shown in (A) while (B) contains only the data obtained between −5 and +5 V. The solid lines are guides to the eye. The vertical dashed line in (B) indicates the built-in voltage of the devices.

H-plasma-treated ITO anode shows no PL quenching upon increasing the voltage from zero to V_{BI}, and only 3% quenching at 4 V. For the single-layer PPV device with a UV/O$_3$-treated ITO anode the PL is quenched slightly at V_{BI}, and by about 9% at 4 V. However, for the double-layer PPV device containing a PEDOT:PSS layer, the PL efficiency at V_{BI} is about 6% lower than that at 0 V, and almost 20% lower at 4 V. Furthermore, the PL efficiency of the double-layer PPV device has a maximum at a negative bias of about −2 V. All results shown in Fig. 3 were reversible, and independent of scan direction.

This paper focusses on the differences in PL quenching at small applied voltages around V_{BI}. For larger applied voltages above V_{BI}, quenching mechanisms connected to the electric field and/or the flow of charge carriers can occur, but such mechanisms will not be elaborated upon in this paper. The differences in PL quenching around V_{BI} cannot be ascribed to field- and/or current-driven mechanisms: quenching is observed below and at V_{BI}, where the internal field is minimal and only very small leakage currents flow. Instead, Fig. 3 points to a decisive role of some type of interaction between the anode and the LEP. This was confirmed by field-dependent PL measurements for unipolar devices with Au cathodes, where a similar degree of quenching around V_{BI} was observed.

The voltage dependence of the PL intensity for various LEP thicknesses is shown in Fig. 4. The left-hand graph shows PL quenching at large reverse voltages. Would the data at reverse voltages be replotted versus applied field, all curves would coincide indicating that the PL quenching scales with the internal field. The right-hand graph focuses on the intensity variations around V_{BI}. It is clearly seen that the degree of quenching at V_{BI} is largest for lower LEP layer thickness. It should also be noted that the intensity for the thicker layers does not show a pronounced PL maximum at negative voltage, as do the curves for the thinner layers. For the 34 nm LEP layer, reverse-field PL quenching occurs already at small negative voltages so that it overwhelms the expected increase of the PL intensity below −2 V.

3.2. Electrical impedance

Electrical impedance spectroscopy is a powerful method to characterize the electrical behavior of a system and to study physical processes occurring at interfaces [23]. A typical measurement on a single-layer device (i.e. a device containing only a LEP layer sandwiched between two electrodes) is shown in Fig. 5, together with the equivalent circuit that is used to fit the data. An equivalent circuit should represent the physical processes taking place, be as simple as possible, yet be able to satisfactorily describe the experimental results.

The equivalent circuit in Fig. 5 consists of a series combination of a contact resistance (R_{c}) and a parallel RC-element. The latter describes the organic layer as being a so-called leaky capacitor. R_{c} does not depend on the dc voltage and typically amounts to 10 Ω. R_1 equals the differential resistance ($\mathrm{d}R = \mathrm{d}V/\mathrm{d}I$) and can also be derived from a dc IV-measurement. C_1 does not depend on the applied voltage and corresponds to the geometrical capacitance (C_0) of the LEP layer ($C_0 = \varepsilon A/d$), where ε is the dielectric permittivity of the LEP

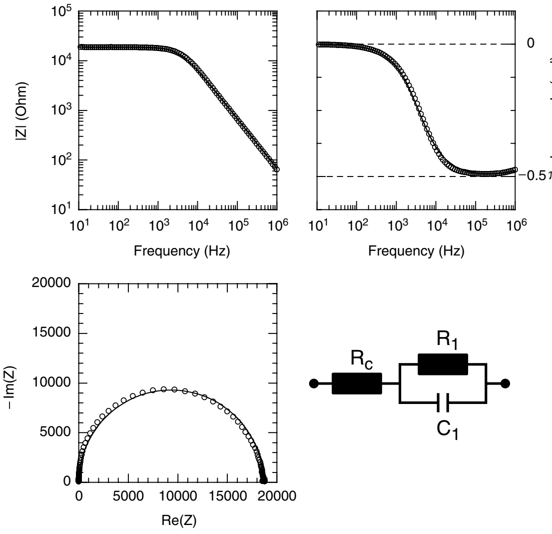

Fig. 5. Impedance measurement on a single-layer device with PPV as LEP (open circles). The measurement was performed at a dc voltage of 4 V. The equivalent circuit shown is used to fit the measurement (solid line).

material, A the diode surface area, and d the layer thickness).

A double-layer device, i.e. containing PEDOT:PSS, shows a more complicated impedance and entirely satisfactory equivalent circuits could not be obtained. The best equivalent circuit at voltages close to or below V_{BI} contains a series combination of two parallel RC-elements and a contact resistance. By comparison to the single-layer device, the capacitance associated with the LEP layer was determined. At voltages well above V_{BI}, the impedance could again be fitted to the simple equivalent circuit shown in Fig. 5.

Fig. 6(A) compares results for single and double-layer devices. For both, the capacitance of the PPV layer at voltages well above V_{BI} is equal to the geometrical capacitance (as measured on a single-layer device). At V_{BI}, however, the capacitance of the PPV layer in a double layer device reaches a maximum. At voltages well below V_{BI}, the capacitance is again independent of the voltage but has a value higher than the geometrical capacitance.

For a bipolar double-layer device containing PSF instead of PPV, the voltage-dependence of the LEP layer capacitance is shown in Fig. 6(B). The same features are present as observed in the corresponding PPV device, with the notable exception of the capacitance maximum at V_{BI}. For both types of devices, the measured capacitance shifts from a certain constant value at voltages lower than V_{BI} to a lower constant value at voltages higher than V_{BI}, the latter being the geometrical capacitance of the LEP layer. Although additional experiments are required to quantify the constant capacitance measured at voltages below V_{BI}, at this moment it is clear that this capacitance is connected to an intrinsic property of the PEDOT:PSS layer and not indicative of an interaction between PEDOT:PSS and LEP. Irrespective of the type of LEP, a shift of the capacitance occurs at V_{BI} when a PEDOT:PSS layer is present in the device (compare Fig. 6(A) and (B), and note the absence of a capacitance shift for a device in which no PEDOT:PSS layer is present).

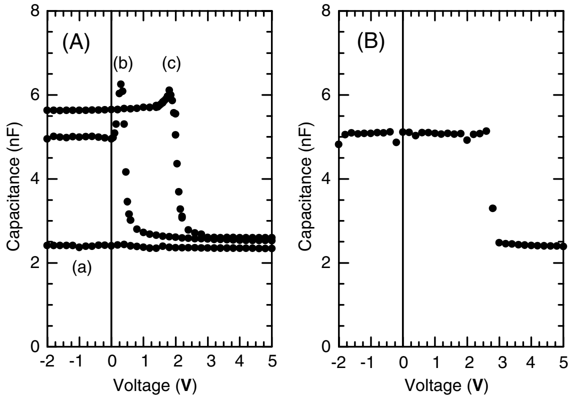

Fig. 6. Dependence of the LEP capacitance on applied voltage for two different polymers: (A) PPV and (B) PSF. For PPV, three different types of devices are shown: (a) unipolar single-layer device, (b) unipolar double-layer device, and (c) bipolar double-layer device. For PSF, only a bipolar double-layer device is shown. For all devices, the LEP layer has a thickness of 120 nm and in the double-layer devices also a PEDOT:PSS layer of 150 nm is present.

The capacitance maximum is also observed for unipolar PPV devices containing PEDOT:PSS. Thus, its occurrence parallels PL quenching of single LEP layers discussed in Section 3.1.1, and PL quenching close to V_{BI}, discussed in Section 3.1.3. The remainder of this discussion will, therefore, focus on the capacitance maximum of the PPV layer at V_{BI} in double-layer devices.

The problem of obtaining a fully satisfactory equivalent circuit for the double-layer pLEDs becomes more evident when the admittance (Y) of the device is plotted. When the diode behaves as a purely parallel RC-element, the imaginary part of the admittance (after correction for the serial contact resistance) equals the angular frequency times the capacitance $(Y \equiv 1/Z = 1/R + \mathrm{i}\omega C)$. The voltage dependence of $\mathrm{Im}(Y)/\omega$ is plotted in Fig. 7, showing a frequency dependence that cannot be described by a purely capacitive behavior. An additional contribution to the admittance at negative bias and a notable peak at V_{BI} are evident for lower frequencies. In the equivalent circuit fits of Fig. 6, this was evident as a small discrepancy between the fitted and measured impedance at low frequency. This indicates that the responsible physical process is relatively slow. For lower frequency, the peak at V_{BI} is only observed for devices containing *both* PPV and PEDOT:PSS. Above V_{BI}, the increasing value of $\mathrm{Im}(Y)\omega$ is due to space-charge limited current flow through the device,

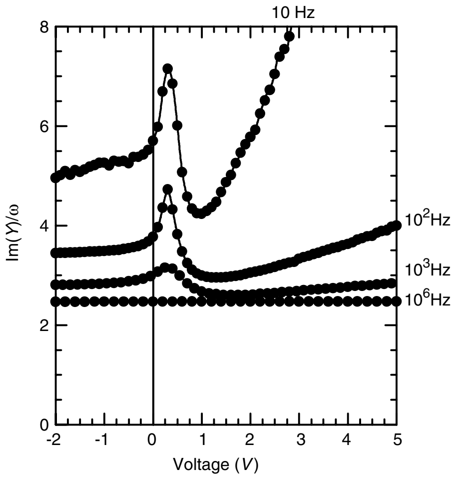

Fig. 7. $\text{Im}(Y)/\omega$ (after correction for a serial contact resistance of 10 Ω) versus voltage for a unipolar double-layer device containing PPV. The measurements are performed at modulation frequencies (f) of 10, 10^2, 10^3 and 10^6 Hz ($\omega = 2\pi f$).

effectively decreasing the thickness of the dielectric layer [24].

4. Discussion

From steady-state PL measurements it is clear that the efficiency of a light-emitting organic compound can suffer from the presence of PEDOT:PSS, depending on the type of compound. This shows that when calculating properties of pLEDs it can be misleading to use quantum efficiencies extracted from measurements on LEP layers on glass or LEP solutions. In the simplest case the LEP layer of a pLED consists of a pristine polymer such as PPV or PSF. In thin films of such soft condensed matter the interactions at the interface regions can completely determine the properties of the material. So it is rather the quantum efficiency of the LEP layer in its environment, i.e. the layer as part of a stack of layers sandwiched between two electrodes, driven at a specific current density and electric field, that has to be taken into consideration when internal device properties are discussed. Already in such a relatively simple system it is an oversimplification to characterize devices with various device structures and under different operating conditions with just a single value for the quantum efficiency of the LEP. This obviously has important implications for those efficiency related issues that are deduced or partly deduced from combined optical and electrical measurements and use the quantum efficiency as an important variable in the calculation, such as e.g. the much debated singlet-to-triplet ratio. It lies therefore at the basis of every device model with predictive value for efficiencies over a range of operating conditions to carefully look into the mutual influence of the constituting layers of the pLED.

In the presence of PEDOT:PSS, both steady-state PL measurements on molecularly doped polymers and field-dependent PL measurements on PPV layers indicate that a region exists where the PL efficiency is changed from its bulk value. This region extends from the boundary between PEDOT:PSS and LEP into the polymer, introducing a gradient in LEP properties. The importance of this gradient on the measured, averaged PL properties obviously decreases as the thickness of the LEP layer increases. Thus, possible errors introduced by uncontrollable variation of the PL quantum efficiency are expected to be minimal in thick devices.

Actually, three more phenomena contribute to the complexity of an absolute determination of the PL quantum efficiency in devices under operating conditions. The first relates to the positional dependence of the radiative and non-radiative decay rates, due to coupling of the dipole oscillator, i.e. the exciton, to the optical mode density [25–27]. For example, the PL quantum efficiency is attenuated close to a metal interface [28]. This presently precludes an absolute determination of the PL quantum efficiency at 0 V in an actual device, as no sufficiently realistic optical model is available to account for such effects. Secondly, the width of the interface region can increase during electrical operation of a pLED, as demonstrated by the results on the triplet emitter quenching. Thirdly, charge carriers can induce PL quenching [29–31]. Fig. 4 showed a small PL decrease above V_{BI} even for the H-plasma treated ITO. This quenching becomes more pronounced for higher voltage, and is attributed to the presence of charge carriers. Their concentration can show strong variation inside the LEP layer, e.g. for space-charge limited currents [32,33], adding a third mechanism behind the positional dependence of the quantum efficiency.

Summarizing, the PL quantum efficiency in an operating pLED can be different from that measured in a pristine layer for various reasons. Their occurrence depends on the neighboring layers in the device and on the type of polymer. Simple measurements such as steady-state PL and voltage-dependent PL can be used to judge the importance of some quenching mechanisms. Indeed, PPV is found to respond markedly different to the presence of PEDOT:PSS than does PSF: for PPV, interaction with PEDOT:PSS results in the creation of quenching sites, a process that is not observed for PSF.

Combination of the data on electrical impedance and PL quenching can shed more light on the nature of the quenching sites. The field-dependent PL measurements are entirely consistent with the electrical impedance data: only those devices that show a considerable attenuation of the PL efficiency at V_{BI}, show a maximum of the LEP layer capacitance at V_{BI}. This behavior is only observed for double-layer devices. Therefore, the presence of PEDOT:PSS is essential in this respect. For pLEDs, a voltage-dependent capacitance has been reported before, for instance in the case of diodes made from precursor PPV [34]. There, the conversion of the precursor leads to the presence of mobile holes in the polymer. Consequently, a Schottky barrier diode is formed with a depletion layer at the cathode interface. The width of this depletion layer, and hence its capacitance, is voltage dependent.

For the experiments described here, the presence of mobile charge carriers in the polymer layer as a result of device fabrication is not to be expected. The presence of a Schottky barrier at the cathode side of the device is unlikely as the current–voltage characteristics depend on the thickness of the LEP layer according to space-charge limited current behavior [32,33,35]. Furthermore, for Schottky barrier diodes an electric field only exists at the polymer–cathode interface and as a result electroluminescence can be observed at relatively low voltages, even when cathodes of high work function metals such as Au are used. This is not observed for our devices. For a double-layer PPV device, the maximum of the PPV layer capacitance at V_{BI} is observed irrespective of the type of cathode used. However, the capacitance maximum is very sensitive towards changes at the anode side of the device. This points out that in our devices the voltage-dependence of the PPV layer capacitance has its origin at the anode side, and there is no Schottky barrier at the cathode side.

The work on precursor PPV does, however, contain an important message for the present discussion: acid is released in the conversion process, which is responsible for the formation of holes. Thus, the capacitance maximum and the field-dependent PL quenching observed in our work are attributed to a voltage-dependent concentration gradient of holes in PPV, in agreement with the decisive role of the anode in both observations, and the unimportance of the type of cathode. The difference between PPV and PSF is ascribed to the sensitivity of the vinylene bond—present in PPV but not in PSF—to acidic substances such as PEDOT:PSS. Quenching sites could then be created in PPV by an electrophilic addition reaction involving the vinylene bond of PPV and protons from PEDOT:PSS.

The states responsible for the PL quenching can be probed with electrical impedance measurements. From the admittance analysis it is clear that the maximum of the PPV layer capacitance at V_{BI} for a double-layer device is present only at low modulation frequency, indicative of a relatively slow physical process. When the quenching sites created in PPV due to the interaction with PEDOT:PSS are capable of trapping charge carriers, the charging of these traps will be visible in an impedance measurement as an increase of the capacitance, as observed in the measurements described in this paper. From a certain threshold voltage onwards, the population of traps at the interface will always be entirely filled and consequently have no effect on the impedance of the device anymore (hence the occurrence of a capacitance maximum).

Field-dependent PL measurements show a maximum of the PL intensity at about −2 V (i.e. well below V_{BI}). As the voltage increases, the PL intensity quenches. In electrical impedance measurements, an increase of the capacitance is only observed just below V_{BI}. This difference in the voltage-dependence of the capacitance and PL is due to the difference in measurement techniques. Measuring the PL is a dc technique and, as such, it measures the cumulative effect of an increasing number of trapped charges present in the LEP when the voltage is increased towards V_{BI}. Due to the exciton diffusion length, quenching of the PL intensity can become noticeable already for a very small concentration of trapped charges. The amount of quenching cannot exceed 100% and, therefore, the decrease in PL intensity will level off once a certain population of traps has been charged. Measuring the electrical impedance is an ac technique and probes the incremental number of charged traps due to an incremental change in applied voltage. Only at applied voltages where a sufficiently large number of traps can be charged/decharged, will the effect on the impedance be noticeable.

For pLEDs it is well known that trapping/detrapping of charge carriers can be a slow process, depending on the depth of the traps involved [36,37]. Already at voltages below V_{BI}, traps in the interface region between PEDOT:PSS and PPV are being charged. In an impedance measurement this manifests itself as an increase of the capacitance while in a field-dependent PL measurement the charging of the traps results in quenching of the luminescence.

5. Conclusions

The experiments described in this paper clearly demonstrate the importance of determining the photophysical and electrical properties of LEPs in actual working devices. Apart from well-known electric field-induced and current-induced luminescence quenching processes, chemical interactions between layers in the light-emitting device can result in the occurrence of additional quenching mechanisms that influence both the host polymer and molecular dopants dispersed in the host. Chemical interactions can be especially important when studying polymer light-emitting diodes that employ PEDOT:PSS as a hole injection layer, depending on the type of LEP that is used. This has important implications for those efficiency related issues that are deduced or partly deduced from combined optical and electrical measurements.

Acknowledgements

The authors would like to thank Covion Organic Semiconductors GmbH for making available the poly-(*p*-phenylenevinylene) and poly-(2,7-spirofluorene) derivatives used for the experiments described in this paper.

References

[1] S. Lamansky, R.C. Kwong, M. Nugent, P.I. Djurovich, M.E. Thompson, Org. Electron. 2 (2001) 53.
[2] J. Morgado, F. Cacialli, R. Iqbal, S.C. Moratti, A.B. Holmes, G. Yahioglu, L.R. Milgrom, R.H. Friend, J. Mater. Chem. 11 (2001) 278.
[3] D.F. O'Brien, C. Giebeler, R.B. Fletcher, A.J. Cadby, L.C. Palilis, D.G. Lidzey, P.A. Lane, D.D.C. Bradley, W. Blau, Synth. Metals 116 (2001) 379.
[4] J.S. Wilson, N. Chawdhury, M.R.A. Al-Mandhary, M. Younus, M.S. Khan, P.R. Raithby, A. Köhler, R.H. Friend, J. Am. Chem. Soc. 123 (2001) 9412.
[5] R.W.T. Higgins, A.P. Monkman, H.G. Nothofer, U. Scherf, J. Appl. Phys. 91 (2002) 99.
[6] V. Cleave, G. Yahioglu, P. Le Barny, R.H. Friend, N. Tessler, Adv. Mater. 11 (1999) 285.
[7] M.A. Baldo, D.F. O'Brien, Y. You, A. Shoustikov, S. Sibley, M.E. Thompson, S.R. Forrest, Nature 395 (1998) 151.
[8] M.A. Baldo, M.E. Thompson, S.R. Forrest, Pure Appl. Chem. 71 (1999) 2095.
[9] S. Lamansky, P. Djurovich, C.E. Murphy, F. Abdel-Razzaq, R.C. Kwong, I. Tsyba, M. Bortz, B. Mui, R. Bau, M.E. Thompson, Inorg. Chem. 40 (2001) 1704.
[10] S. Lamansky, P. Djurovich, D. Murphy, F. Abdel-Razzaq, H.E. Lee, C. Adachi, P.E. Burrows, S.R. Forrest, M.E. Thompson, J. Am. Chem. Soc. 123 (2001) 4304.
[11] M. Goes, J.W. Verhoeven, H. Hofstraat, K. Brunner, Chem. Phys. Chem. 4 (2003) 349.
[12] Y. Cao, G. Yu, C. Zhang, R. Menon, A.J. Heeger, Synth. Metals 87 (1997) 171.
[13] L. Groenendaal, F. Jonas, D. Freitag, H. Pielartzik, J.R. Reynolds, Adv. Mater. 12 (2000) 481.
[14] H. Spreitzer, H. Becker, E. Kluge, W. Kreuder, H. Schenk, R. Demandt, H. Schoo, Adv. Mater. 10 (1998) 1340.

[15] H. Becker, H. Spreitzer, W. Kreuder, E. Kluge, H. Schenk, I.D. Parker, Y. Cao, Adv. Mater. 12 (2000) 42.

[16] H. Becker, A. Büsing, A. Falcou, S. Heun, E. Kluge, A. Parham, P. Stößel, H. Spreitzer, K. Treacher, H. Vestweber, Proc. SPIE 4464 (2001) 49.

[17] D.R. Lide (Ed.), CRC Handbook of Chemistry and Physics, 73rd ed., CRC Press, Boca Raton, USA, 1992–1993.

[18] B.H. Cumpston, I.D. Parker, K.F. Jensen, J. Appl. Phys. 81 (1997) 3716.

[19] M. Goes, Photo- and Electroluminescence Generated by Intramolecular Charge Transfer, Ph.D. Thesis, University of Amsterdam, Amsterdam, 2002.

[20] R. Kersting, U. Lemmer, M. Deussen, H.J. Bakker, R.F. Mahrt, H. Kurz, V.I. Arkhipov, H. Bässler, E.O. Göbel, Phys. Rev. Lett. 73 (1994) 1440.

[21] V.I. Arkhipov, H. Bässler, M. Deussen, E.O. Göbel, R. Kersting, H. Kurz, U. Lemmer, R.F. Mahrt, Phys. Rev. B 52 (1995) 4932.

[22] M.C.J.M. Vissenberg, M.J.M. de Jong, Phys. Rev. Lett. 77 (1996) 4820.

[23] J.R. MacDonald, Impedance Spectroscopy. Emphasizing Solid Materials and Systems, John Wiley & Sons, New York, 1987.

[24] H.C.F. Martens, H.B. Brom, P.W.M. Blom, Phys. Rev. B 60 (1999) R8489.

[25] H. Kuhn, J. Chem. Phys. 53 (1970) 101.

[26] R.R. Chance, A. Prock, R. Silbey, J. Chem. Phys. 62 (1975) 2245.

[27] R.R. Chance, A. Prock, R. Silbey, J. Chem. Phys. 65 (1976) 2527.

[28] H. Kurczewska, H. Bässler, J. Lumin. 15 (1977) 261.

[29] P. Dyreklev, O. Inganäs, J. Paloheimo, H. Stubb, J. Appl. Phys. 71 (1992) 2816.

[30] E.J.W. List, C.H. Kim, A.K. Naik, U. Scherf, G. Leising, W. Graupner, J. Shinar, Phys. Rev. B 64 (2001) 155204.

[31] R.H. Young, C.W. Tang, A.P. Marchetti, Appl. Phys. Lett. 80 (2002) 874.

[32] P.W.M. Blom, M.J.M. de Jong, IEEE J. Sel. Top. Quantum Electron. 4 (1998) 105.

[33] P.W.M. Blom, M.C.J.M. Vissenberg, Mater. Sci. Eng. R 27 (2000) 53.

[34] M. Meier, S. Karg, W. Riess, J. Appl. Phys. 82 (1997) 1961.

[35] M.A. Lampert, P. Mark, Current Injection in Solids, Academic Press, New York, 1970.

[36] P.H. Nguyen, S. Scheinert, S. Berleb, W. Brütting, G. Paasch, Org. Electron. 2 (2001) 105.

[37] G. Paasch, S. Scheinert, Synth. Metals 122 (2001) 145.